

# Single-photon two-qubit SWAP gate for entanglement manipulation

Marco Fiorentino,\* Taehyun Kim, and Franco N. C. Wong

*Research Laboratory of Electronics, Massachusetts Institute of Technology, Cambridge, MA 02139*

A SWAP operation between different types of qubits of single photons is essential for manipulating hyperentangled photons for a variety of applications. We have implemented an efficient SWAP gate for the momentum and polarization degrees of freedom of single photons. The SWAP gate was utilized in a single-photon two-qubit quantum logic circuit to deterministically transfer momentum entanglement between a pair of down-converted photons to polarization entanglement. The polarization entanglement thus obtained violates Bell's inequality by more than 150 standard deviations.

PACS numbers: 03.67.-a, 03.67.Lx, 42.50.Dv, 03.67.Mn

Linear optical quantum computation (LOQC) has recently attracted great interests following the demonstration [1] that a scalable quantum computer based on linear optical components is possible. It has also been known that linear optical systems could achieve non-scalable quantum computation by encoding multiple qubits in several degrees of freedom of a single photon [2]. Experiments in the latter were limited to a few qubits due to the complexity of the optical setup [3] and they did not use entanglement resources. Recently, however, several groups have proposed the use of deterministic logic gates in conjunction with sources of entangled or hyperentangled (i.e., entangled in more than one degree of freedom) photons to execute simple quantum protocols. The combination of deterministic logic and entangled photons can be used for one-shot demonstration of nonlocality with two observers [4], complete measurement of Bell's states [5], cryptographic protocols [6], and quantum games [7]. These proposed experiments rely on the ability to create hyperentangled states and successively project them onto suitable sets of basis states for measurement. Manipulation of entanglement would benefit significantly from efficient deterministic one- and two-qubit gates thus permitting hyperentangled photons to be used as essential quantum resources.

In the case of hyperentanglement in the polarization and momentum (spatial) degrees of freedom of a single photon, single-qubit rotation can be accomplished using wave plates and beam splitters. We have recently demonstrated a single-photon two-qubit (SPTQ) implementation of a deterministic controlled NOT (CNOT) gate that operates on the momentum and polarization degrees of freedom of single photons [8]. It is well known that any arbitrary unitary operation can be generated using CNOT gates and single-qubit rotations, which can be used to manipulate qubits of single or entangled photons. In this letter we apply SPTQ logic to manipulate entanglement between two photons. Specifically, we have built a SWAP gate and transferred the entanglement in the momentum degree of freedom of a pair of

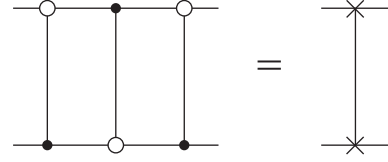


FIG. 1: Schematic of the SWAP gate logic circuit.

down-converted photons to their polarization. This type of transfer is fundamentally different from “entanglement swapping” as described in Ref. [9]: our SWAP operation involves two different qubits of the same photon, whereas conventional entanglement swapping is between the same type of qubit of two different photons. Our experiment is both the first application of SPTQ logic to entangled photons and a verification of the momentum entanglement of down-converted photons. Compared to similar proposals [4, 5] our implementation of SPTQ logic has the advantage of relying on gates that are robust and require no active path length stabilization, therefore simplifying the optical layout. The ability to swap two qubits constitutes an important step toward the realization of proposed SPTQ protocols [4, 5, 6, 7]. For example, some single-qubit operations necessary to implement these protocols, such as single-qubit rotations and projections onto the  $(|0\rangle + |1\rangle, |0\rangle - |1\rangle)$  basis, require phase-stable interferometers for the momentum qubit. With the SWAP gate, one can implement these operations in the polarization domain simply with wave plates and polarizers.

For the quantum resource in our experiment we exploit the intrinsic momentum entanglement of down-converted photon pairs. This type of entanglement has been demonstrated by Rarity and Tapster [10] and is based on the conservation of momentum in the parametric down-conversion process. The state of the down-conversion output can be derived from Eq. 7 in Ref. [11]. For simplicity we assume the pump to be a monochromatic plane wave propagating along the crystal's principal  $x$  axis. The state is given by

$$|\Psi\rangle_{IN} \simeq \int d\mathbf{q}_S d\omega_S L e^{-i\frac{L\Delta}{2}} \text{sinc}\left(\frac{L\Delta}{2}\right) \hat{a}_H^\dagger(\mathbf{q}_S, \omega_S) \hat{a}_V^\dagger(-\mathbf{q}_S, \omega_P - \omega_S) |0\rangle, \quad (1)$$

\*Electronic address: mfiore@mit.edu

where the integral is a triple integral that extends to the whole plane spanned by the transverse (with respect to  $x$ ) component  $\mathbf{q}_S$  of the signal wavevector and over the range of positive frequencies spanned by the signal frequency  $\omega_S$ . The creation operators refer to the horizontally ( $H$ ) and vertically ( $V$ ) polarized signal and idler, respectively.  $L$  is the crystal length,  $\omega_P$  is the pump frequency, and  $\Delta$  is the phase mismatch as defined in Ref. [11]. Equation (2) shows the correlation in momentum between signal and idler photons. We now restrict our attention to two propagation directions: one on the top  $\mathbf{q}_T$  and its conjugate at the bottom  $\mathbf{q}_B = -\mathbf{q}_T$ . We take the signal frequency to be  $\omega_S = \omega_P/2$  and assume the phase mismatch  $\Delta$  to be zero. In the experimental setup the single frequency and single direction constraints were enforced by the use of interference filters and irises. The state then becomes

$$|\Psi\rangle_{IN} \simeq \left( \hat{a}_H^\dagger(\mathbf{q}_T, \omega_P/2) \hat{a}_V^\dagger(\mathbf{q}_B, \omega_P/2) + \hat{a}_H^\dagger(\mathbf{q}_B, \omega_P/2) \hat{a}_V^\dagger(\mathbf{q}_T, \omega_P/2) \right) |0\rangle. \quad (2)$$

Equation (2) describes two photons that can be in four orthogonal states: horizontally polarized top ( $HT$ ), vertically polarized top ( $VT$ ), horizontally polarized bottom ( $HB$ ), and vertically polarized bottom ( $VB$ ). Each photon is therefore described by a state in a four dimensional Hilbert space. Following Ref. [4] we rewrite each four-dimensional Hilbert space as the tensor product of two two-dimensional Hilbert spaces (i.e. qubits). In this formalism the normalized state (2) can be rewritten as

$$\begin{aligned} |\Psi\rangle_{IN} &= \frac{1}{\sqrt{2}}(|T_S B_I\rangle + |B_S T_I\rangle) \otimes |H_S V_I\rangle \\ &\equiv \frac{1}{\sqrt{2}}(|0_{MS} 1_{MI}\rangle + |1_{MS} 0_{MI}\rangle) \otimes |0_{PS} 1_{PI}\rangle, \end{aligned} \quad (3)$$

In the final expression we identify the  $H$  and  $T$  states with the logical 0 and the  $V$  and  $B$  states with the logical 1 for the four qubits designated as polarization ( $P$ ) and momentum ( $M$ ) of the signal ( $S$ ) and idler ( $I$ ). From Eq. 4 it is clear that the photons emitted by the crystal are not polarization entangled in general, unless signal and idler photons are indistinguishable spectrally (frequency degenerate) and temporally (timing compensated) [12, 13], in which case the  $T$  and  $B$  beams are polarization entangled, as demonstrated in Ref. [14]. In the present experiment we ensure that the photons are not polarization entangled by not compensating the birefringence-induced time delay.

Manipulation of the four-qubit state of Eq. 4, two for each photon, can be achieved using SPTQ logic. We have previously demonstrated a high fidelity polarization-controlled NOT (P-CNOT) gate for SPTQ logic [8] by use of a polarization Sagnac interferometer with an embedded dove prism that flips and rotates the input beam by  $90^\circ$ . A momentum-controlled NOT (M-CNOT) gate can be realized with a half-wave plate (HWP) oriented at  $45^\circ$  relative to the horizontal position and inserted in

the path of the  $B$  beam. The SWAP we present here is a more complex quantum gate that can be obtained by applying three consecutive CNOT gates [15] as shown in Fig. 1. A SWAP gate exchanges the values of two arbitrary qubits without the need of measuring them. For example, when applied to the arbitrary two-qubit *product* state  $(\alpha|T\rangle + \beta|B\rangle) \otimes (\gamma|H\rangle + \delta|V\rangle)$  a SWAP gate transforms it into the state  $(\gamma|T\rangle + \delta|B\rangle) \otimes (\alpha|H\rangle + \beta|V\rangle)$ . Note that a SWAP acting on a qubit that is part of an entangled pair of qubits transfers the entanglement to the other qubit, which may be more conveniently manipulated. In the case of hyperentangled photons, for example, swapping the entanglement from the momentum to the polarization qubit allows a complete and unequivocal proof of the successful generation of hyperentanglement. In our logic protocol applying a sequence of a M-CNOT followed by a P-CNOT and another M-CNOT realizes a SWAP gate. A SWAP gate applied to both photons in the initial state  $|\Psi\rangle_{IN}$  yields the polarization-entangled state

$$|\Psi\rangle_{OUT} = \frac{1}{\sqrt{2}}|0_{MS} 1_{MI}\rangle \otimes (|0_{PS} 1_{PI}\rangle + |1_{PS} 0_{PI}\rangle). \quad (4)$$

Observe that if we omit the last M-CNOT gate the output state is

$$|\Psi'\rangle_{OUT} = \frac{1}{\sqrt{2}}|0_{MS} 1_{MI}\rangle \otimes (|0_{PS} 0_{PI}\rangle + |1_{PS} 1_{PI}\rangle). \quad (5)$$

which is also polarization entangled. Signal and idler photons in  $|\Psi\rangle_{OUT}$  and  $|\Psi'\rangle_{OUT}$  are in a definite momentum state (signal and idler are on opposite sides). Therefore they can be separated with a mirror that reflects one part of the beam and not the other. It is worth noticing that the entanglement swapping presented here is deterministic, i.e., in principle all the momentum-entangled photon pairs are converted into polarization-entangled pairs.

Figure 2 shows our experimental setup. We used pairs of down-converted photons from a 1-cm-long periodically poled potassium titanyl phosphate (PPKTP) crystal that was continuous-wave pumped at 398.5 nm for type-II phase-matched frequency-degenerate parametric down-conversion [12]. The crystal temperature was adjusted so that signal and idler photons were emitted in two overlapping cones with an external full divergence of  $\sim 13$  mrad. The momentum modes were chosen with two apertures after the gates instead of a two-hole aperture mask placed before the gate as was done in Ref. [8]. We observed a higher gate fidelity with the separate apertures after the gates, probably due to slight size mismatch of the two-hole mask. In our experimental realization of entanglement swapping we used the same physical gates to manipulate both photons of the pair. The two photons crossed the gates at different times owing to the delay accumulated in the PPKTP crystal and therefore no interference between them took place. The M-CNOT gate was a HWP cut in a half-circular D shape with the fast axis forming a  $45^\circ$  angle with the  $H$  direction. The plate

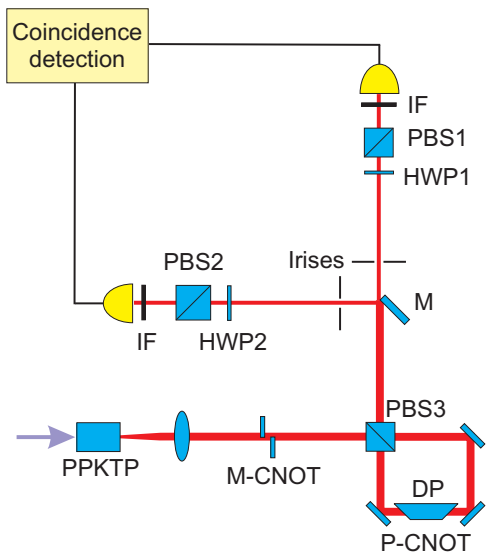


FIG. 2: Schematic of experimental setup. PPKTP: periodically poled KTP crystal. PBS: polarizing beam splitter. DP: dove prism. HWP: half-wave plate. IF: 1-nm interference filter. M: mirror. P-CNOT: polarization-controlled NOT gate. M-CNOT: momentum controlled NOT gate.

was aligned so that it only affected the bottom section of the beam. A second HWP, identical to the first except for the fact that its axis was parallel to the  $H$  axis, was put in the path of the top part of the beam to compensate for the time delay introduced by the first HWP. The compensating wave plate was slightly tilted to obtain optimal visibility in the entangled state analysis. This tilting changed the length of the top beam path thus allowing one to correct for path mismatch. The P-CNOT gate was a polarization Sagnac interferometer with an embedded dove prism [8]. The input polarizing beam splitter (PBS3) of the P-CNOT gate directed horizontally (vertically) polarized input light to travel in a clockwise (counterclockwise) direction. As viewed by each beam, the dove prism orientation was different for the two counter-propagating beams. Therefore the top-bottom ( $T$ - $B$ ) sections of the input beam were mapped onto the right-left ( $R$ - $L$ ) sections of the output beam for  $H$ -polarized light but onto the  $L$ - $R$  sections for  $V$ -polarized light. If we identify  $|H\rangle$ ,  $|T\rangle$ , and  $|R\rangle$  with the logical  $|0\rangle$  and  $|V\rangle$ ,  $|B\rangle$ , and  $|L\rangle$  with the logical  $|1\rangle$  it is easy to recognize that this setup implements a CNOT gate in which the polarization is the control qubit and the momentum (or spatial) mode is the target qubit. After the P-CNOT gate the state of the photon pair is described by Eq. 5; we separated signal and idler photons using the mirror  $M$  shown in Fig. 2 that reflected only the right section of the beam. Signal and idler beams were then separately sent through a 2.2-mm iris, a polarization analyzer formed by a HWP and a polarizer, and a 1-nm interference filter centered at 797 nm. Besides being used for polarization analysis, wave plate HWP2 in Fig. 2 assumed the role of the second M-CNOT gate, thus completing the SWAP

circuit. The photons were detected with single-photon counting modules (PerkinElmer SPCM-AQR-14) and we measured signal-idler coincidences through a fast AND gate with a 1-ns coincidence window [16]. Given the short coincidence window and the observed count rates (singles rates  $\leq 100,000$  counts/s), accidental coincidences were negligible.

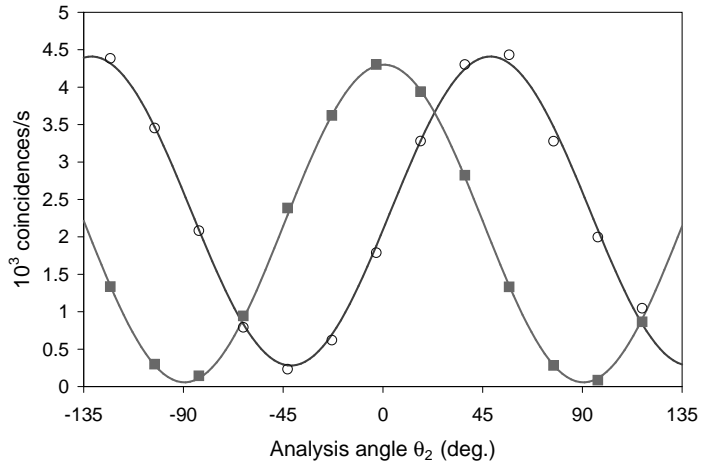


FIG. 3: Coincidence rates as a function of the polarization analysis angle  $\theta_2$  in arm 2 when the analyzer in arm 1 was set at an angle  $\theta_1 = 0^\circ$  (solid squares) and  $45^\circ$  (open circles). The lines are sinusoidal fits to the data.

To test the performance of the SWAP gate we analyzed the resultant polarization entanglement. Figure 3 shows the coincidence rates versus the polarization analysis angle  $\theta_2$  in arm 2 of Fig. 2 when the analyzer in arm 1 was set at  $0^\circ$  (solid squares) and  $45^\circ$  (open circles). The visibility of the sinusoidal fits is  $V_0 = 97 \pm 2\%$  for  $0^\circ$  data and  $V_{45} = 88 \pm 2\%$  for the  $45^\circ$  data. The difference in visibility is due to the fact that  $V_{45}$  is more sensitive than  $V_0$  to the imperfections of the source and the gate interferometer. A measurement of the S parameter [17] for the Clauser-Horne-Shimony-Holt form of the Bell's inequality gives a value of  $2.653 \pm 0.004$  that violates the classical limit of 2 by more than 150 standard deviations. These results clearly show that our SWAP gate had a good fidelity and that the down-converted photons were indeed initially momentum entangled.

The  $V_{45}$  results in Fig. 3 include errors due to imperfect interference at the gate (gate fidelity) and incomplete momentum entanglement of the source (source fidelity). To determine how well our setup approximates the ideal SWAP gate it is useful to separate the two contributions. As a test we sent an attenuated laser beam (filtered through a single-mode fiber and collimated with an aspheric lens) through the gate, with the laser frequency being the same as that of the down-converted photons. By injecting the laser with a linear polarization oriented at  $45^\circ$  relative to the  $H$  direction we measured the classical visibility of the SWAP gate. This test measurement gave a visibility  $V_{C1}$  of  $\sim 93\%$  for the gate. We also verified that the M-CNOT gate did not affect

the classical visibility in a measurable way. The classical measurement was repeated without the dove prism in the polarization Sagnac interferometer (of the P-CNOT gate) that yielded a visibility  $V_{C2}$  of  $\sim 95\%$ . The 2% difference in the classical visibility ( $V_{C1} - V_{C2}$ ) can be attributed to either imperfections in the dove prism or asymmetries in the injected laser beam. To further evaluate the cause, we repeated the test experiment with a polarization Sagnac interferometer in a triangular configuration that was insensitive to input beam asymmetry. In this configuration the interference at the  $T$  position at the output originated from the same spot of the injected beam for both polarizations, with or without the dove prism (and similarly for the  $B$  position at the output). For the triangular configuration we obtained a difference in classical visibility with and without the dove prism of  $\sim 2.5\%$  that is comparable to that of the non-triangular configuration, indicating that the dove prism was responsible for a loss of  $\sim 2\%$  in the visibility of the P-CNOT gate. The remaining  $\simeq 5\%$  loss of classical visibility  $V_{C1}$  can be attributed to wavefront distortions introduced by the beam splitter cube (which leads to our continuing effort to obtain a polarizing beam splitter with a low wavefront distortion in both transmission and reflection). Given our quantum visibility  $V_{45}$  of 88% and the classical test measurement results of the P-CNOT interferometer we conclude that the source fidelity was 95% that was limited by imperfections in the momentum entanglement

of the down-conversion source (probable causes: defects in PPKTP crystal poling and wavefront distortions of the downconverted beams). The SWAP gate fidelity was 93% and was limited by less than ideal components (polarizing beam splitter and dove prism).

In conclusion we have demonstrated a high fidelity SWAP gate for single-photon two-qubit logic. To realize such a gate we have built an essential set of gates in the SPTQ quantum logic family comprising linear optical P-CNOT and M-CNOT gates that are robust and do not need active length stabilization. We applied the SWAP gate to momentum-entangled photons thereby transferring the entanglement from the momentum to the polarization degree of freedom. This is, to the best of our knowledge, the first application of SPTQ linear optical quantum logic to entangled photons. Our experiment opens the way to the demonstration of more complex SPTQ manipulation of entanglement including the manipulation of 3- and 4-photon states. This type of few-qubit quantum information processing is at the core of a number of applications ranging from single-shot two-observers demonstration of nonlocality [4] to two-qubit quantum key distribution [6].

This work was supported by the the DoD Multidisciplinary University Research Initiative (MURI) program administered by the Army Research Office under Grant DAAD-19-00-1-0177.

- 
- [1] E. Knill, R. Laflamme, and G. J. Milburn, *Nature* **409**, 46 (2001).
- [2] N. J. Cerf, C. Adami, and P. G. Kwiat, *Phys. Rev. A* **57**, R1477 (1998); J. C. Howell and J. A. Yeazell, *Phys. Rev. A* **61**, 052303 (2000); B. G. Englert, C. Kurtziefer, and H. Weinfurter, *Phys. Rev. A* **63**, 032303 (2001).
- [3] P. G. Kwiat, J. R. Mitchell, P. D. D. Schwindt, and A. G. White, *J. Mod. Opt.* **47**, 257 (2000); Y. Mitsumori, J. A. Vaccaro, S. M. Barnett, E. Andersson, A. Hasegawa, M. Takeoka, and M. Sasaki, *Phys. Rev. Lett.* **91**, 217902 (2003).
- [4] Z.-B. Chen, J.-W. Pan, Y.-D. Zhang, C. Brukner, and A. Zeilinger, *Phys. Rev. Lett.* **90**, 160408 (2003).
- [5] S. P. Walborn, S. Pádua, and C. H. Monken, *Phys. Rev. A* **68**, 042313 (2003).
- [6] M. Genovese and C. Novero, *Eur. Phys. J. D* **21**, 109 (2002).
- [7] K.-Y. Chen, T. Hogg, and R. Beausoleil, *Quant. Info. Proc.* **1**, 449 (2002).
- [8] M. Fiorentino and F. N. C. Wong, *to appear in Phys. Rev. Lett.* and quant-ph/0402208.
- [9] J.-W. Pan, D. Bouwmeester, H. Weinfurter, and A. Zeilinger, *Phys. Rev. Lett.* **80**, 3891 (1998).
- [10] J. G. Rarity and P. R. Tapster, *Phys. Rev. Lett.* **64**, 2495 (1990).
- [11] M. Atatüre, G. Di Giuseppe, M. D. Shaw, A. V. Sergienko, B. E. A. Saleh, and M. C. Teich, *Phys. Rev. A* **66**, 023822 (2002).
- [12] C. E. Kulewicz, M. Fiorentino, G. Messin, F. N. C. Wong, and J. H. Shapiro, *Phys. Rev. A* **69**, 013807 (2004); M. Fiorentino, G. Messin, C. E. Kulewicz, F. N. C. Wong, and J. H. Shapiro, *Phys. Rev. A* **69**, 041801(R) (2004).
- [13] M. H. Rubin, D. N. Klyshko, Y. H. Shih, and A. V. Sergienko, *Phys. Rev. A* **50**, 5122 (1994).
- [14] P. G. Kwiat, K. Mattle, H. Weinfurter, A. Zeilinger, A. V. Sergienko, and Y. Shih, *Phys. Rev. Lett.* **75**, 4337 (1995).
- [15] M. A. Nielsen and I. L. Chuang, *Quantum Computation and Quantum Information* (Cambridge University, Cambridge, 2000) p. 23.
- [16] T. Kim, M. Fiorentino, P. V. Gorelik, and F. N. C. Wong, “Low-cost nanosecond electronic coincidence detector,” submitted to *Rev. Sci. Instrum.*
- [17] J. F. Clauser, M. A. Horne, A. Shimony, and R. A. Holt, *Phys. Rev. Lett.* **23**, 880 (1969); A. Aspect, P. Grangier, and G. Roger, *Phys. Rev. Lett.* **49**, 91 (1982).